DOI: 10.13009/EUCASS2025-547
11TH EUROPEAN CONFERENCE FOR AERONAUTICS AND SPACE SCIENCES (EUCASS)

DEVELOPMENT AND TESTING OF AN ADDITIVELY MANUFACTURED COUNTER-SWIRL INJECTOR HEAD

Markus Ortelt[1], Markus Selzer[1], Helge Seiler[1]

[1]*Instiute of structures and design, German Aerospace Centre, Stuttgart, Germany*

Markus.Ortelt@dlr.de, https://www.dlr.de/en/bt

Abstract

Additive manufacturing allows for new designs for injection elements of rocket engines. Counter-swirled injection channels of different sizes can be integrated in each injection element. Additionally, using an integrated design reduces time consuming integration steps.
On the other hand, additive manufacturing of these features requires extensive knowledge during the manufacturing process to make sure the single channels all function as intended.
Therefore, cold spray tests on single injector elements have been conducted using H20 and gaseous nitrogen as test fluids. Functionality of different channel sizes, pressure loss and spray characteristics have been evaluated during these tests and are described in this paper.

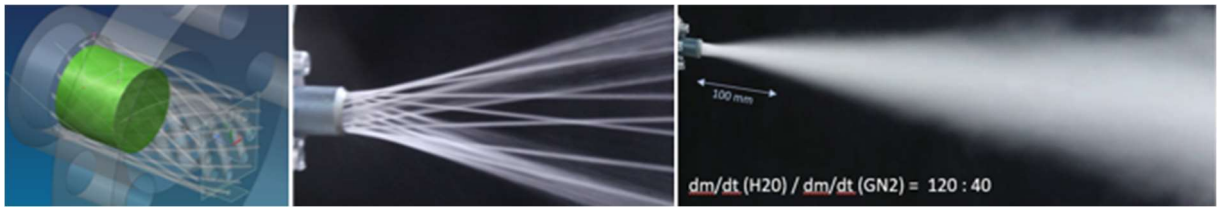

Figure 1 : CAD of the swirl channel design (left), resulting spray pattern using water (middle) and spray behavior (right)

The findings of these tests resulted in the design and additive manufacturing of a full-size injector head featuring 24 injection elements as shown in *Figure 2*.


Figure 2 : Additively manufactured swirl-injector head

In the paper, the following magnitudes are used: Re – Reynolds-Number; ρ - density; v – velocity; d – diameter; μ - dynamic viscosity; λ – pipe-friction-coefficient; k – roughness and individually defined constant in flow-spin equation; $\dot{m}$ – mass flow; $\dot{V}$ – volume flow; L – length; s – distance; α, β - angels; $\dot{\varphi}$ -angular velocity; A – cross-section area.

DOI: 10.13009/EUCASS2025-547

1. Introduction

Since more than two decades DLR develops transpiration cooled CMC thrust chambers for high performance rocket engines. The latest demonstrator design focus' a 60 kN LOx/LCH4 operation as a representative size for flexible new space applications. The demonstrator shows an inner diameter of 116 mm in the cylindrical combustion chamber zone and a sub-sonic chamber length of 400 mm. The defined overall mass flow amounts to approx. 19.6 kg/s at a mixture ratio of 3.3. The injector-O/F amounts to approx. 3.9, so that most of the excess fuel (approx. 0.8 kg/s) will be used as coolant diffused through the inner homogeneously micro-porous CMC combustion chamber wall. A brief functional and structural overview is given in Figure *3*.

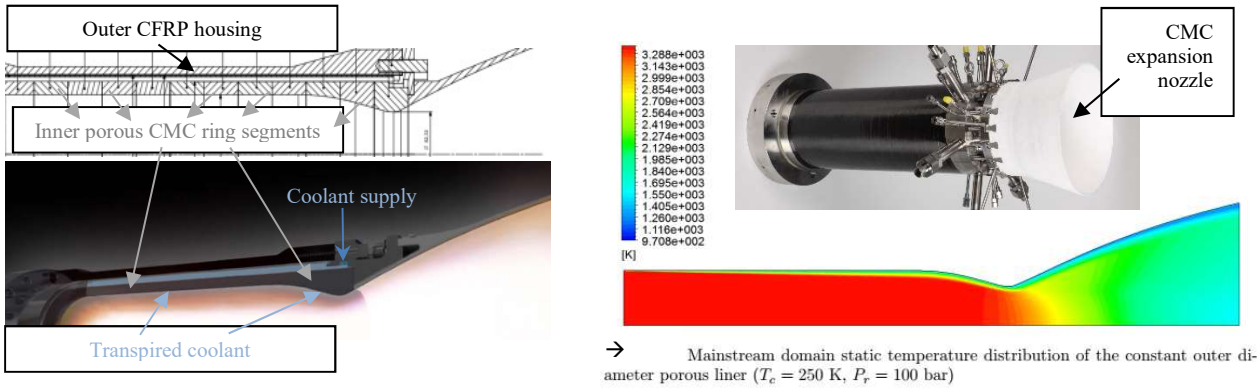

→ Mainstream domain static temperature distribution of the constant outer diameter porous liner ($T_c = 250$ K, $P_r = 100$ bar)

Figure 3 : Functional overview of the transpiration cooled CMC combustion chamber. CFX-analysis without combustion (right)

The inner CMC ring segments will be stacked one to each other like a stack of pineapple slices, where the fiber-plies of the composite material itself are oriented perpendicular-wise related to the chamber axis. The latter gives on the one hand the coolant a radial preferred diffusional direction towards the combustion space. On the other hand, the mechanical ring-stack allows a very flexible arrangement of potentially completely different ring segments. This means, that e.g. the ring-thickness can be varied to allow different diffusion intensities for optimized out-blowing cooling profiles along the hot-gas flow in the combustion chamber, or, that a variety of inherent physical and thermo-chemical material properties can be adjusted according to wall-protecting mechanisms adjacent to the inner hot-gas surface.

The major technological goal on injector side is a good mixing of the propellants to get a possibly fine spray pattern of small droplets. The finer the ejected propellant droplets, the lower is the risk of attacking the combustion chamber wall surface by e.g. oxygen-rich hot spots, leading to thermo-chemical surface damage. For that reason, the transpiration cooling will already have been initiated, when igniting the ejected mixed propellants, and, the transpiration mechanism stops after shut-down of the combustion as well. Hence, the inner wall surface will be protected in every critical operational phase (Figure 4).

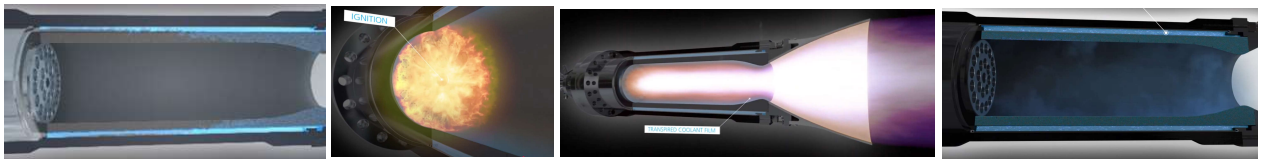

Figure 4 : Wall transpiration is activated before ignition (a), during ignition (b), during steady-state operation (c) and after extinction (d)

2. New injector head component

The global shape of the new injector head component is depicted in Figure 2. It consists of a cylindrical basic body, that has been manufactured additively with Inconel 718 powder on an EOS facility at DLR Cologne. The outer contours have been finished by classical manufacturing methods like turning and grinding, implementing the required surface quality and interface tolerances. Inside the component, there are two manifolds, one for LOx and one for LCH4. Due to homogeneous supply conditions, there are six supply pipes welded on the outer cylindrical surface for both propellants, each in a circular star array. The shapes of the inside manifold walls of the injector component orient on maximum printable overhang angles around 50°, so that the raw component can be printed fully in one procedure.

DOI: 10.13009/EUCASS2025-547

2.1 Array of injector elements on the faceplate

The injector mass flow is distributed onto 24 single elements. The single elements are arrayed in three rows with diameters I, II and III (*Figure 5*).

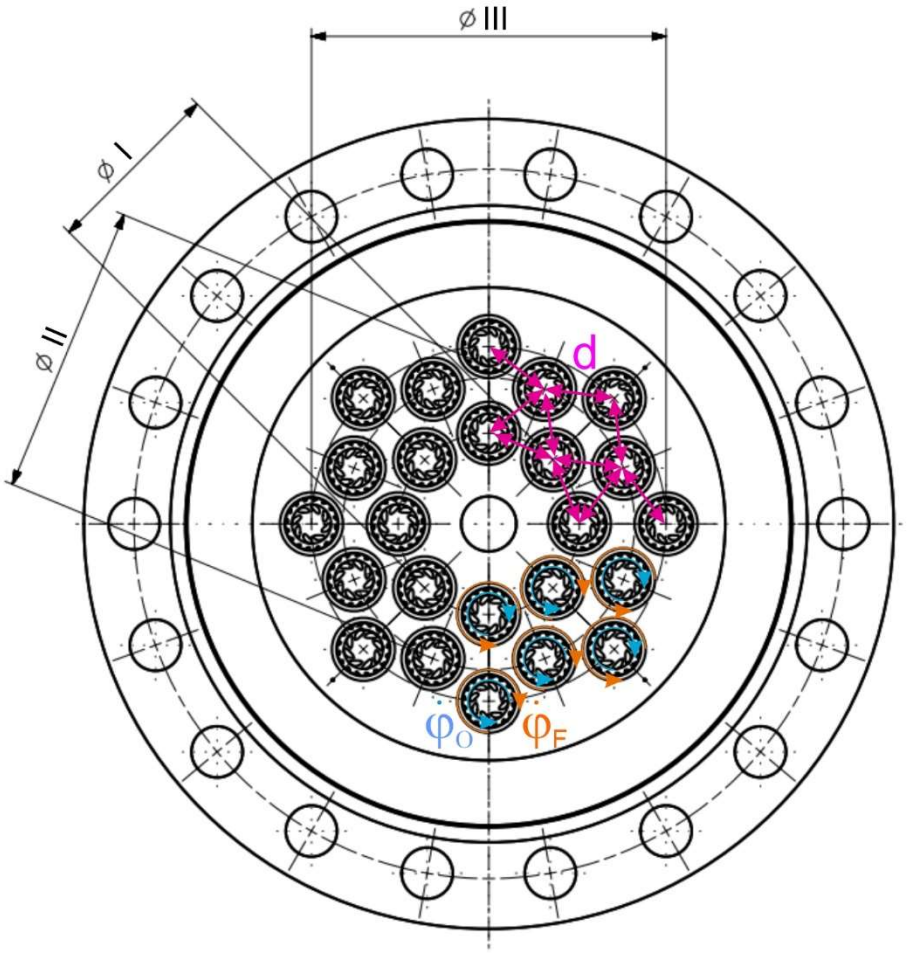

Figure 5 : Element pattern of the counter-swirl injector head component.

The intension of the array is having almost equal distance d between elements of adjacent rows. To generate swirled impinging mechanism between oxidizer and fuel, each element shows different spin-direction of LOx-channels and LCH4-channels, leading to counter-wise rotational speeds $\dot{\varphi}_O$ and $\dot{\varphi}_F$. Additionally, the elements themselves show alternating rotational directions, for balancing reasons of the global ejection spin. The latter means, that same numbers of elements swirl in both directions.

2.2 Description of one representative single injector element

Each single element shows 8 channels for the LOx ejection, and 16 channels for LCH4 in counter-wise spin orientation. The ejection angles α and β are geometrically defined by planar unwinding of the spiral channel centre lines as given in *Figure 6*. These angles will be defined by the final flow-spin balance in combination with the propellant densities and ejection speeds.
In case of LOx / LCH4 use, the recess of the LOx outlet will be twice compared to the LCH4 recess RC. The circular outlet face for LOx shows a diameter of 12 mm, adjusted to the channel distribution for the required LOx mass flow of the 60 kN design, given above.

DOI: 10.13009/EUCASS2025-547

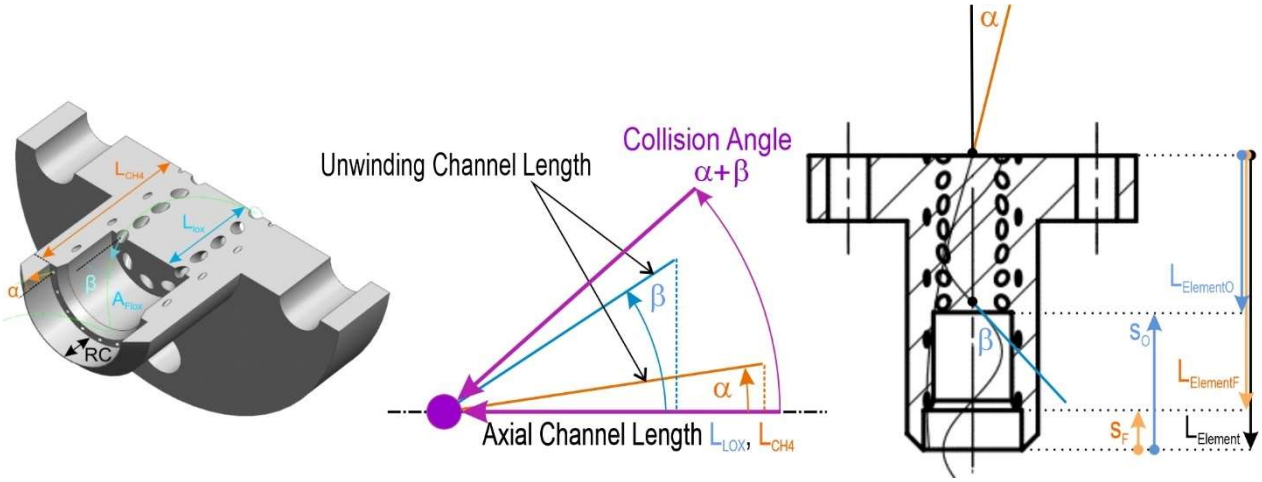

Figure 6 : Shape of the single injector element and construction of the collision angle between LOx- and LCH4 ejection jets.

2.3 Assessment of flow-friction inside the ejection channels

Before designing the final channel geometry, the flow friction inside the ejection channels had to be been assessed. For that reason, the roughness of the inner channel surface has been measured at representative test specimens by a KEYENCE VR-5000 device (*Figure 7*). Different types of hole geometry have been investigated at three channel-rows A, M and I, and as realistically estimated average values of the surface roughness were taken to evaluate the channel flow (k = 0.0001 m). The minimum diameter of the smaller LCH4 ejection channels has been chosen to be 0.6 mm.

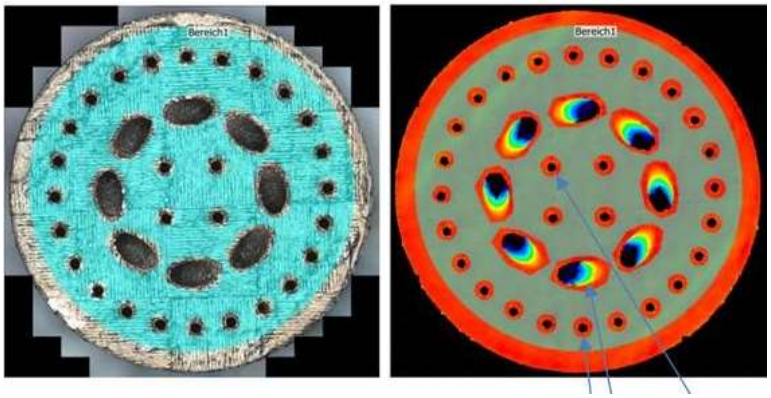

Analysis Properties					
Roughness Standard	ISO 25178-2:2012				
Filter Type	Gauß				
S-Filter	No				
F-Process	No				
L-Filter	No				
End-Correction	Active				
Results	Sa	Sz	Str	Spc	Sdr
	µm	µm		1/mm	-
Max.	29,271	429,800		50,726	0,1655718
Min.	29,271	429,800		50,726	0,1655718
Average	29,271	429,800		50,726	0,1655718
Standard Deviation	0.000	0.000		0,000	0,0000000
Section 1	29,271	429,800		50,726	0,1655718

Figure 7 : Diagnostical evaluation of surface roughness by a KEYENCE VT-5000 device.

To get a starting solution for the channel geometry, the friction parameters for LOx and LCH4 in the channels have been calculated preliminarily by an online-calculator [66]. The corresponding friction parameters were iterated in combination with the use of the Moody-diagram.

The following assumptions have been made on an analytical way, to get a starting value for the coefficient of friction. Three equations were used. Firstly, the Reynold's Number (equation 1)

$$Re = \frac{\rho \cdot v \cdot d}{\mu} \tag{1}$$

secondly the hydraulic roughness by Nikuradse (equation 2)

$$\frac{1}{\sqrt{\lambda}} = -2\log_{10}\left(\frac{k}{3{,}71D}\right) \tag{2}$$

DOI: 10.13009/EUCASS2025-547

and thirdly the Bernoulli-equation for pipe friction (equation 3)

$$\lambda \cdot \frac{\rho \cdot v^2}{2 \cdot d} = \frac{\Delta p}{l} \qquad \rightarrow \qquad \lambda = \frac{2 \cdot \Delta p}{l} \cdot \frac{d}{\rho \cdot v^2} \tag{3}$$

Table 1 summarizes the most important fluid-dynamic parameters, referred to the potential LCH4 flow.

Table 1: Element-specific fluid-dynamic parameters

	k	**d**	**l**	**v**	**μ**	**λ**
Value	0.0001	0.002	0.03	54.763	0.000225	0.043
	m	m	m	m/s	Pa · s	-

Figure 8 shows the coefficient of friction given in the Moody diagram.

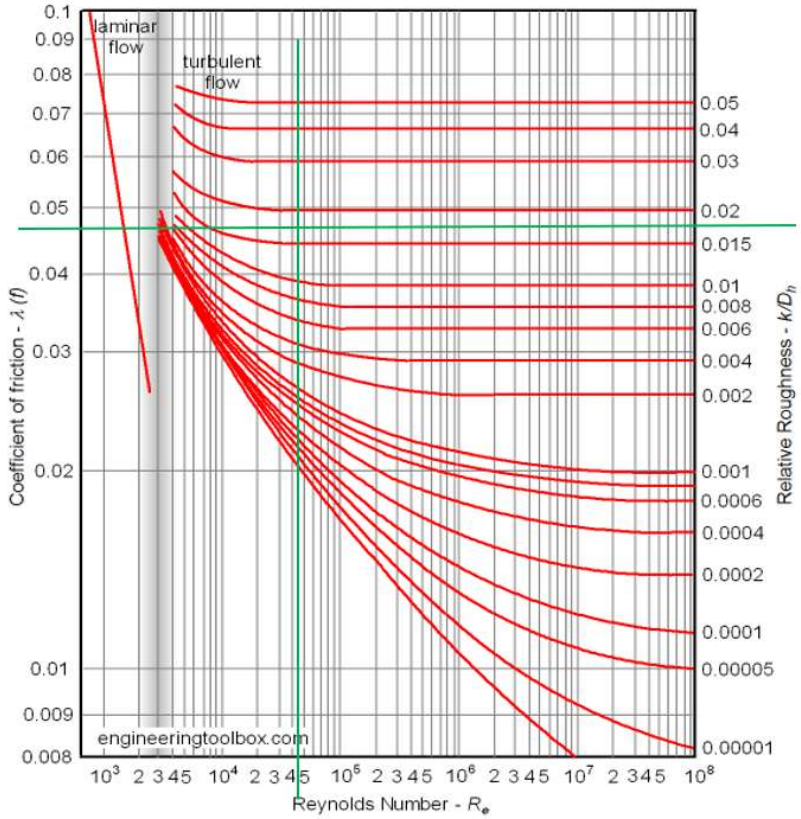

Figure 8 : Moody diagram with preliminarily estimated coefficient of friction (green marks).

Preliminary and subsequent considerations of the general functionality of rocket injectors are and will be related to the references [1÷65]. The new injector element concept here, intends primarily phenomenological investigations and the attempt to find firstly new individual characterization methods, that shall be correlated to the state-of-the-art later.

DOI: 10.13009/EUCASS2025-547

3. Functional requirements

The goal of the spray formation is the assumed balance of both propellant flow-spins inside the injector element. In case this balance is fulfilled, the spray divergence angle decreases to a minimum value, resulting in an optimum of compact and fine spray pattern, represented by the optimum flow-spin-ratio I = 1, derived via equations 4 ÷ 8. The defining characteristics are given in Table *2*. Hereby, the constant C is defined by $C = A_{Element} \cdot \rho$.

$$\dot{V} = \frac{\dot{m}}{\rho} \tag{4}$$

$$v = \frac{\dot{V}}{A_{Element}} \tag{5}$$

$$\dot{m} \cdot v = \rho \cdot v \cdot \dot{V} = \rho \cdot A_{Element} \cdot v^2 = C \cdot v^2 \tag{6}$$

$$k = \frac{C_{LCH4}}{C_{LOX}} \quad \rightarrow \quad (0.0793414) \tag{7}$$

$$\boldsymbol{I = k \cdot \frac{v_{LCH4}^2}{v_{LOX}^2} \overset{!}{=} 1} \tag{8}$$

Table 2: Characteristic flow parameters

	LCH4	**LOx**
Element cross section area [mm^2]	4.832	22.682
Density [kg/m^3]	431.55	1158.7
Constant C [10^{-6} kg/m]	2085.25	26281.98
α [°]	16	-
β [°]	-	42
v_{LCH4} [m/s]	59.11	-
v_{LOX} [m/s]	-	16.26

In this development state the influence of the viscosity has preliminarily being excluded.

4. First preliminary assessment of the spray patterns

The experimental proof of flow-spin-ratio optimum at I = 1 was provided by an extended series of tests, using one representative single injector element (see Figure *6*). Both circuits, the one for LOx and the other for LCH4 in this demonstrator element, have each been flowed through with both water and gaseous nitrogen, to observe their individual outflow behaviour.

DOI: 10.13009/EUCASS2025-547

In a second stage, the mixture of water in LOx-channels and GN2 in the LCH4-channels has been conducted. The observation of the spray formation stood in the focus, or the variation of spray formation respectively.
But firstly, the friction behaviour has been optimized by iterated friction parameters.

4.1 Iterated friction parameters

The measured data of pressures and mass flows provided optimized estimation of channel friction. Using Bernoulli equation (3), a more realistic friction number λ could be derived, and consequently a more realistic friction parameter k could be iterated from the Moody diagram (see Figure *9*, bottom). This new parameter k represents additionally the influence of the helix-geometry of the channels, why it is called 'virtual' friction parameter k. The results show sufficient accuracy of data points for design purpose. Remark: In the evaluated test data, a slight influence of Δp_{Supply} has been considered (Figure *9*, top and Figure *10*).

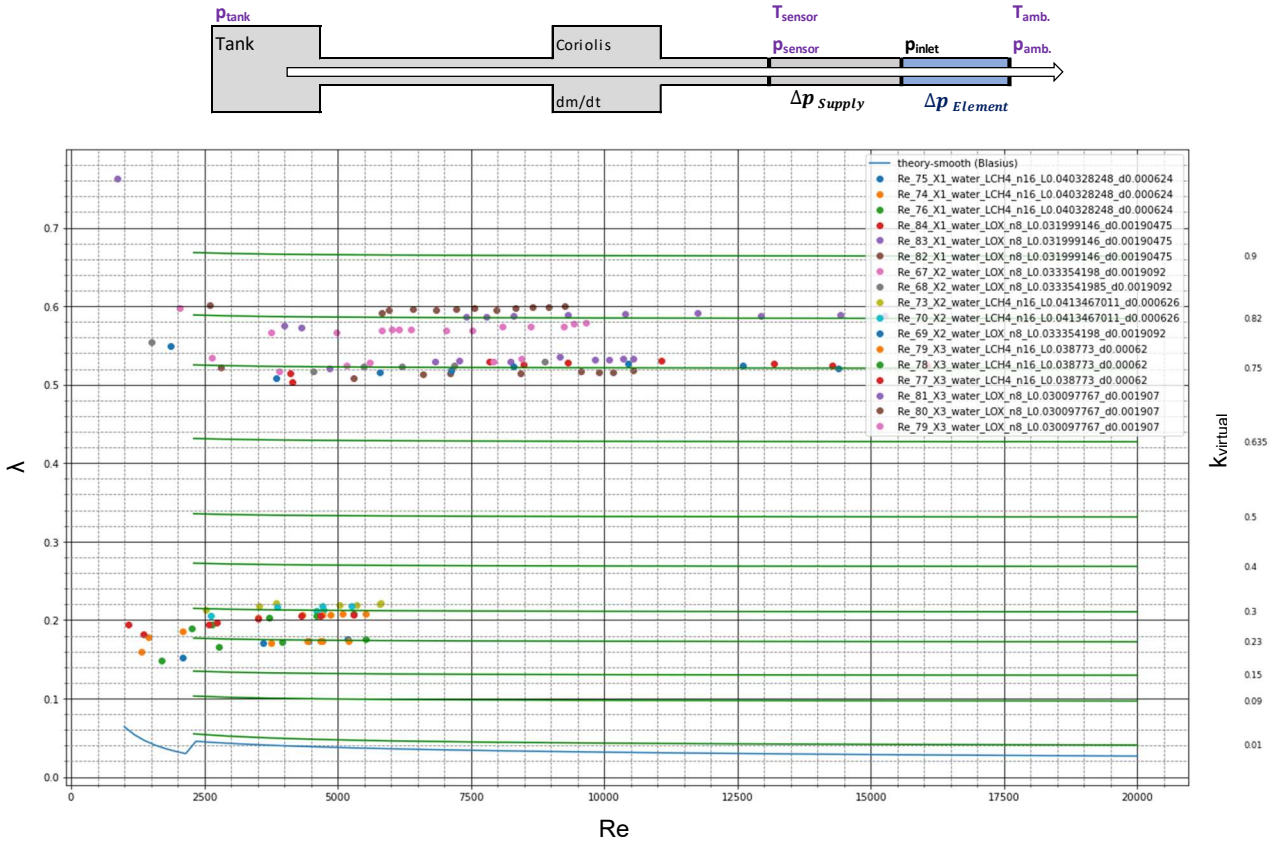

Figure 9 : Sketch of flow chain in the tests (top); Iterated 'virtual' friction parameters k, considering also the helix-geometry of the channels, derived from measurement (bottom).

Three different geometric element configurations X1, X2 and X3 have been tested (see Figure *6* and Table *3*):

Table 3: Geometric element variation

Geometric element type	**X1***	**X2***	**X3***
$L_{Element}$ = **const. = L**	**L**	**L**	**L**
Recess s_O	**L - $L_{ElementO-X1}$**	**L - $L_{ElementO-X2}$**	**L - $L_{ElementO-X3}$**
Recess s_F	**L - $L_{ElementF-X1}$**	**L - $L_{ElementF-X2}$**	**L - $L_{ElementF-X3}$**
s_O **-** s_F **= const. =** **Δs**	**Δs**	**Δs**	**Δs**

* X2: short recess; X1: medium recess; X3: long recess (recess difference from one to the other: 1mm)

DOI: 10.13009/EUCASS2025-547

Finally, it was decided to use the medium recess X1 value in the injector head component.

The pressure loss in the media supply has been considered by the results given in Figure *10*.

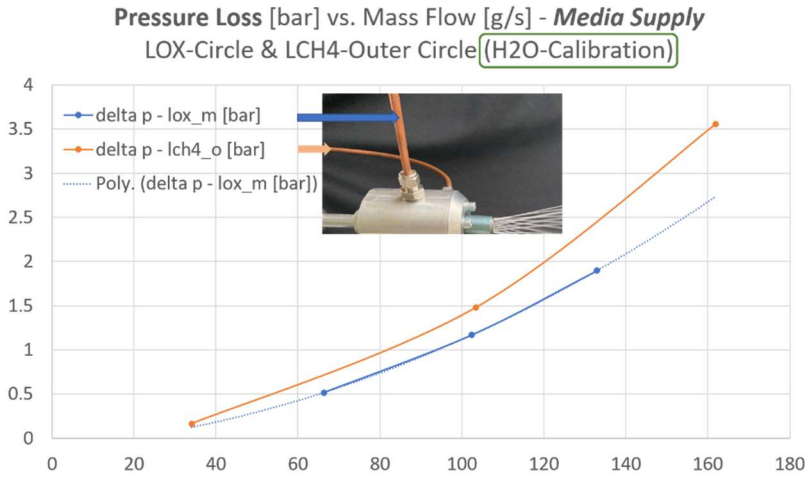

Figure 10: Measurement of pressure loss in the media supply.

4.2 Correlation of operational parameters and spray patterns

Before evaluating the patterns of mixed sprays, firstly the flow through both circuits, LOX and LCH4 channels with pure osmotic water should show, how the media leave the element. Figure *11* and Figure *12* show the water flow through the LOx channels and through the LCH4 channels with increased speed. Figure *11* shows the ejection of water at relevant mass-flow level related to the real LOx-flow simulation.

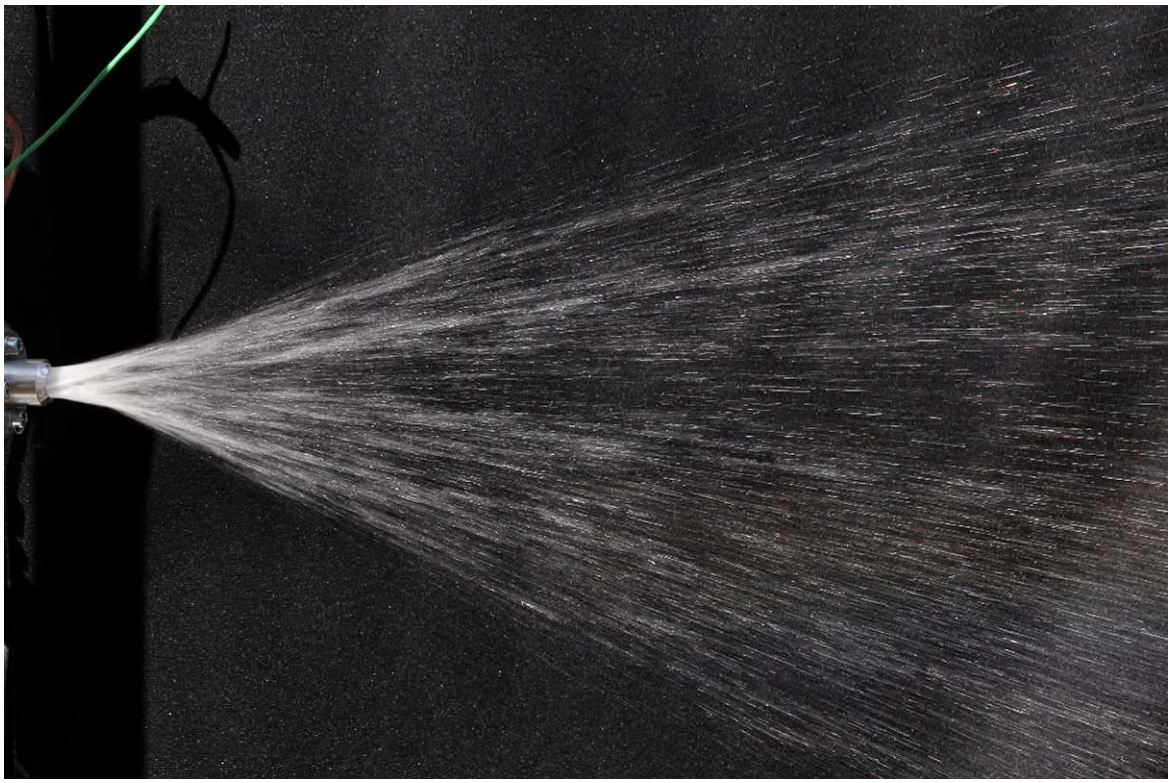

Figure 11: Pure water flow through LOx channels with increased speed at relevant mass-flow level for LOx simulation.

DOI: 10.13009/EUCASS2025-547

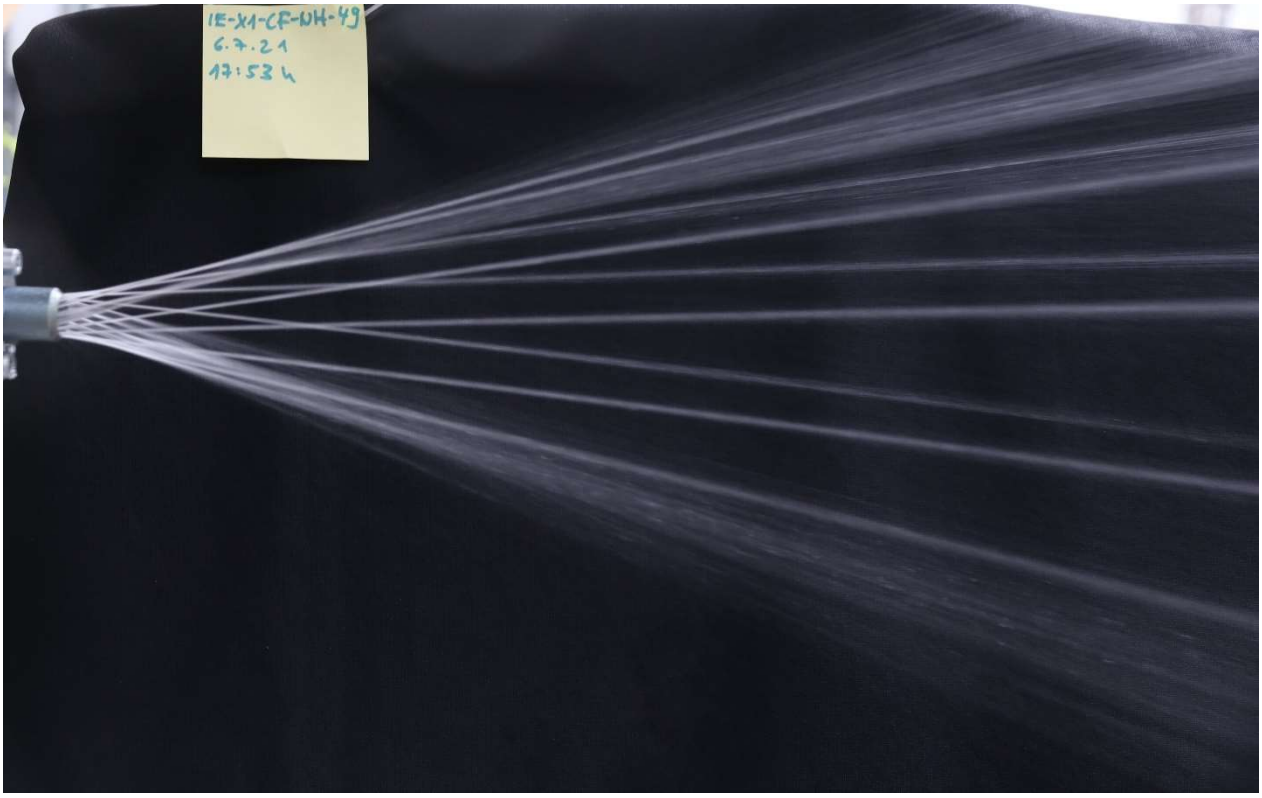

Figure 12: Pure water flow through LCH4 channels with increased speed.

The following figures show spray patterns at different I-Numbers, and they give a first idea of spray-cone-divergence depending on the I-Number, as shown with the yellow marked divergence angles in the figures. The spray seems to converge best at around I = 1. *Table 4* shows a comparison of four GN2-Water-tests at different supply conditions and their corresponding I-Numbers.

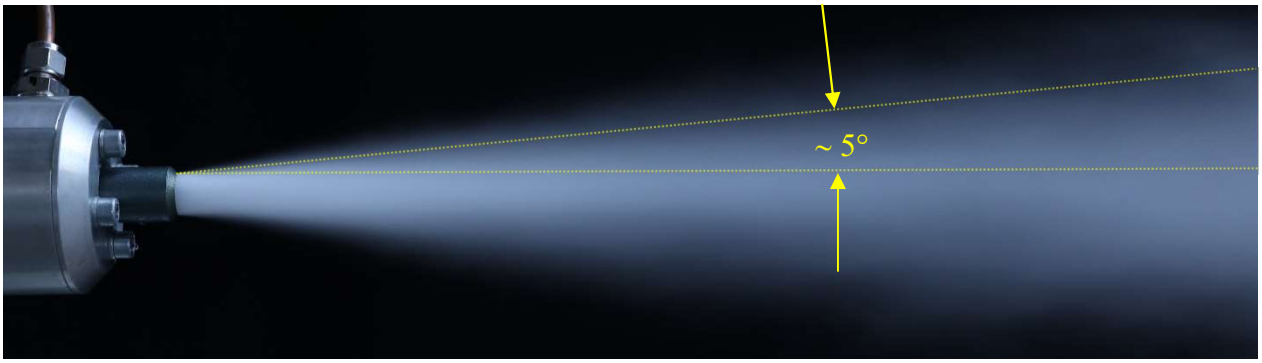

Figure 13: Flow-spin-ratio I = 1.99, closest to the optimum I = 1 (test # IE-X1-CF-HN-53).

DOI: 10.13009/EUCASS2025-547

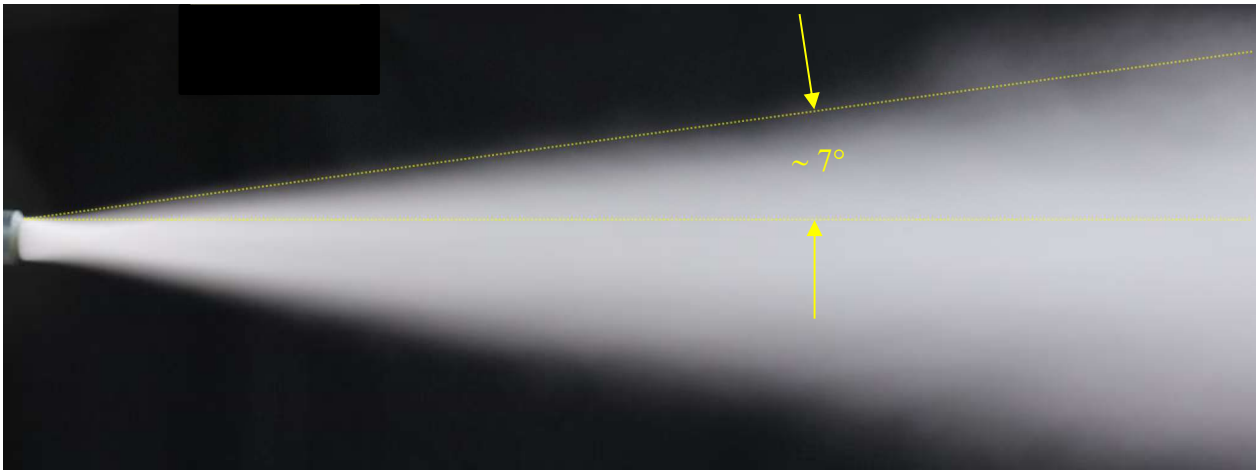

Figure 14: Spray pattern at I = 19.5 (test # IE-X1-CF-HN-46).

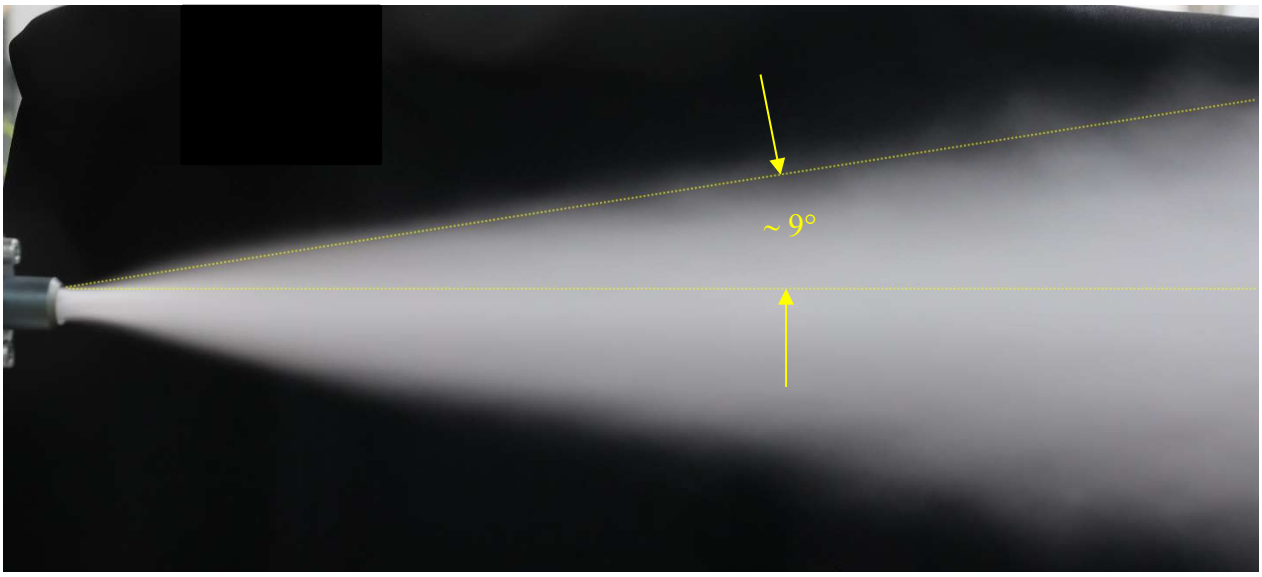

Figure 15: Spray pattern at I = 30.6 (test # IE-X1-CF-HN-48a).

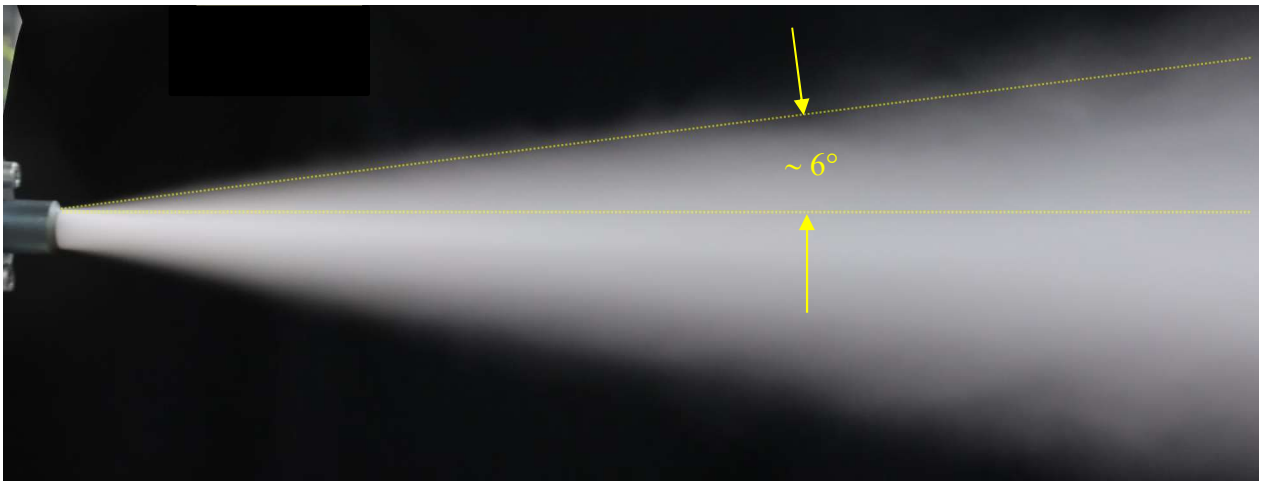

Figure 16: Spray pattern at I = 4.34 (test # IE-X1-CF-HN-48b).

DOI: 10.13009/EUCASS2025-547

As initially described before, Table *4* shall give an overview of test-sets with significantly different I-numbers. The corresponding mass-flow values are related to one single element.

Table 4: Flow parameters of representative tests (with corresponding test identifiers)

	$\dot{m}_{LOx-Channel}$	$\dot{m}_{LCH4-Channe}$	$\Delta p_{LOx-Supply}$	$\Delta p_{LCH4-Supply}$	I
IE-X1-CF-HN-53	150.2	24.4	4.45	53.9	1.99
IE-X1-CF-HN-46	42.2	18.5	0.38	40.0	19.5
IE-X1-CF-HN-48-a	48.8	40.1	0.63	90.4	30.6
IE-X1-CF-HN-48-b	118.9	33.2	2.8	72.6	4.34
	g/s	g/s	bar	bar	-

5. Summary and conclusion

Caused by significant structural manufacturing improvements by the Additive Manufacturing (AI) methods, in particular SLM (Selective Laser Melting), the above described and inherently complex counter-swirl injector-element design can be realized without bigger problems. Considering the knowledge about geometric accuracy at small scales, as well as about tolerances and printable contour angles generally, AI opens excellent opportunities in complex structure manufacturing today, even using metals. Hence, the described counter-swirl injector brought accurate printing results, proved by printing two identical injector-head components, showing similar tolerance accuracy. Choosing 0.6 mm as minimum inner diameter of the ejection-channels, granted for totally open channels, particularly considering the helix-shape of the holes.
According to the given mass-flows rates of the propellants per injector element, the geometric channel shapes have preliminarily been estimated and iterated by checking the flow parameters with an online flow-friction tool, considering mainly the influence of friction.
In the second step, a first set of single injector elements had been manufactured and tested with water and GN2, showing minimum diameters of partially smaller than 0.5 mm. After realizing the minimum acceptable inner channel diameter of 0.6 mm, a second set of injector elements were produced to perform the final single-injector-element pre-tests.
The most accurate spray-forming operation was expected to amount to the flow-spin-balance $I = 1$. The experiments predict cautiously, that actually at $I = 1$ a good mixture and the straightest ejection jets could be observed, whereas I does not include the influence of viscosity yet.
Concerning throttability, it has to be considered additionally to keep the I-Number well-balanced during transient power adjustments in the engine by accurate flow-spin-control.

6. Outlook

The influence of viscosity will be investigated in the next development phase. Additionally, both integral injector head-components will be checked by spraying water and GN2. The transient start-up sequence shall be investigated in a coming spray-test campaign, using firstly water and GN2.
In parallel, first flow-checks with the use of original propellants, LOx and LCH4, will be prepared.